CCS Chemistry

COMMUNICATION

Received: Jan. 24, 2022 | Accepted: Feb. 24, 2022 | Published: Mar. 29, 2022

Mechanistic Insight into Supramolecular Polymerization in Water Tunable by Molecular Geometry

Fan Xu[1], Stefano Crespi[1†], Lukas Pfeifer[1†], Marc C. A. Stuart[1] & Ben L. Feringa[1,2*]

[1]Stratingh Institute for Chemistry, University of Groningen, Groningen 9747 AG, [2]Key Laboratory for Advanced Materials and Joint International Research Laboratory of Precision Chemistry and Molecular Engineering, Feringa Nobel Prize Scientist Joint Research Center, Frontiers Science Center for Materiobiology and Dynamic Chemistry, Institute of Fine Chemicals, School of Chemistry and Molecular Engineering, East China University of Science and Technology, Shanghai 200237

**Corresponding author: b.l.feringa@rug.nl;* [†]Stefano Crespi's present address is: Ångstrom Laboratory, Department of Chemistry, Uppsala University, Uppsala 751 20. Lukas Pfeifer's present address is: Laboratory of Photonics and Interfaces, Department of Chemistry and Chemical Engineering, École Polytechnique Fédérale de Lausanne, Lausanne CH-1015.

Cite this: *CCS Chem*. **2022**, 4, 2212–2220
DOI: 10.31635/ccschem.022.202201821

Supramolecular self-assembly in water based on non-covalent bonding is attracting major attention due to the potential of hydrogels and aqueous polymers in biomedical applications. Although supramolecular polymerization in organic solvents is well established, the key design features, the assembly mechanisms in water and achieving control over the aggregate structures remain challenging. Here, we present the assembly and disassembly of geometrical isomers of a stiff-stilbene bis-urea amphiphile (SA) in pure water. A remarkable feature of this system is that the (*E*)-isomer forms supramolecular polymers in both pure water and organic solvents. Taking advantage of this unique property, the hydrophobic effect was studied by comparing the supramolecular assembly in both systems. The assembly process in water follows an enthalpy-driven nucleation-elongation (cooperative) supramolecular polymerization mechanism with a standard Gibbs free energy ($\Delta G°$ = –53 kJ mol^{-1}) double the value of the one found in toluene. We attributed this distinctive feature to the hydrophobic effect in water. Furthermore, we discovered an isomer-dependent assembly process, which can be used to control aggregation in aqueous media. Due to the substantial geometric difference between (*E*)-SA and (*Z*)-SA, we compared their assembly in water to study the influence of different driving forces involved in the process. The supramolecular polymerization of (*E*)-SA was cooperatively influenced by hydrogen bonding, π-stacking, and hydrophobic effects, whereas the assembly of (*Z*)-SA was mainly driven by hydrophobic effects. As a result, the fiber length of (*E*)-SA in water is much longer than that of (*Z*)-SA, presenting opportunities for geometrical control of aggregation in aqueous media.

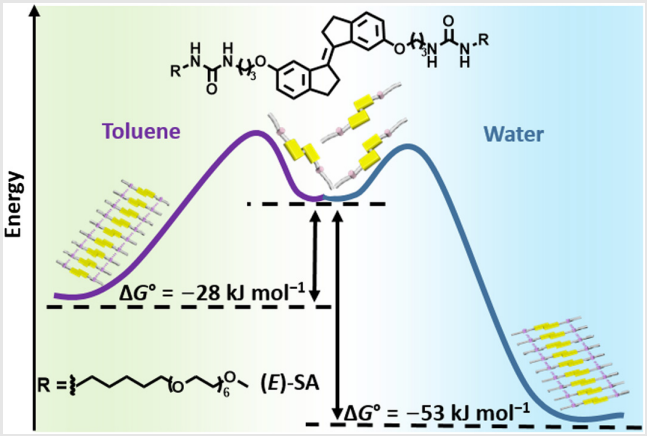

Keywords: supramolecular polymerization, stiff-stilbene, bis-urea, hydrogen bonding, π-stacking, hydrophobic effects

DOI: 10.31635/ccschem.022.202201821
Citation: *CCS Chem*. **2022**, 4, 2212–2220
Link to VoR: https://doi.org/10.31635/ccschem.022.202201821

Introduction

Supramolecular polymers are highly ordered assemblies held together by non-covalent bonds.[1-7] The reversible interaction between their monomers confers bountiful potential to these supramolecular polymers as smart materials, opening new avenues and fascinating opportunities, ranging from material recycling to biomedical applications.[3,8-11] The mechanism of solute-solute interactions in these assemblies is well-established,[1,2,4] whereas the solute-solvent interplay has recently attracted the interest of supramolecular chemists.[12-14] Water is a unique medium for self-assembly in nature, and many exquisite assemblies,[15-24] low-molecular-weight gels,[25-29] and supramolecular polymers[30-36] have been developed in aqueous media for various applications, such as biomolecular materials[37,38] and soft actuators.[39-41] However, detailed insight into supramolecular polymerization in water is far from being as well understood as it is in organic solvents.[12,14] Equally challenging is elucidating the structural features to enable control over the aggregates in water.

Forming supramolecular polymers in aqueous media requires a delicate design of the amphiphilic monomers: the balance of hydrophilicity and hydrophobicity and sufficient directional interactions (non-covalent bonding) to induce the formation of linear supramolecular polymers instead of micellar aggregates.[32,42,43] It is notoriously challenging to study the thermodynamic features of supramolecular polymerization by temperature-dependent experiments due to the strong hydrophobicity of the monomers when exposed to water.[44-46] The principal methods used to investigate the thermodynamic properties of supramolecular polymers in water are computational simulations or inferring conclusions from the assembly in water-organic solvent mixtures.[46-50] Meijer and coworkers revealed that hydrogen bonding controls the directional growth of supramolecular polymers in water using molecular dynamics (MD) simulations.[49] Würthner and coworkers studied the thermodynamic signature of a π-amphiphile, oligo(ethylene glycol) (OEG) functionalized perylene bisimides, in a water/tetrahydrofuran mixture, revealing an entropically-driven assembly process.[46] Interestingly, its analog characterized by a methylene spacer between the perylene bisimide core and the phenyl substituent bearing the OEG followed enthalpy-driven self-assembly in water.[45] The resulting aggregates show opposite reactions to temperature changes: heating induces aggregation in the former structures, whereas the latter assemble during cooling.[45,46] These studies indicate that minimal changes in the molecular structure resulted in fundamentally different assembly processes.[45-47,51-53] Noting the delicate and multiparameter nature of the assembly in water, the question of how hydrogen bonding, π-stacking, and hydrophobic effects cooperatively affect supramolecular polymerization remains largely unanswered. We are also particularly interested in how geometrical changes can affect the assembly.

Stiff-stilbene is a five-membered ring analog of stilbene[54] used for various applications, for example, switchable receptors and ligands,[55-58] force probes,[59] and aggregation-induced emission.[60] The C–Ph torsion angle of the (*E*)-isomer is nearly zero,[61] imposing a planar π system and facilitating the formation of supramolecular assemblies,[54,62-64] whereas the (*Z*)-isomer loses this planarity.[65] The huge geometric differences between (*E*)- and (*Z*)-isomers offer the opportunity to study the influence of π–π interactions on supramolecular polymerization.[64] Recently, we reported a photoinduced cooperative supramolecular polymerization of stiff-stilbene bis-ureas in toluene by taking advantage of the geometric differences and changes in the intramolecular and intermolecular hydrogen-bonding between isomers.[63]

In this study, we investigated the assembly and disassembly of a photoswitchable stiff-stilbene bis-urea amphiphile (**SA**) in pure water. We compared the experimental thermodynamic parameters of its assembly process in water and toluene to gain insights into the role of hydrogen bonding, π-stacking, and hydrophobic effects in supramolecular polymerization in water (Figure 1). (*E*)-**SA** showed the rather unique ability to form supramolecular polymers both in organic solvents and pure water. To the best of our knowledge, limited studies focus on both water and organic solvent-adaptive supramolecular polymers[66]; hence, our present findings provide an excellent opportunity to compare the assembly processes in these distinct environments with the additional benefit that the geometry of the amphiphile can be controlled on demand with light.

Results and Discussion

To study the assembly behavior of **SA** (see Supporting Information Figures S10–S16 for NMR and high resolution MS data)in pure water, we monitored changes in the UV–vis absorption spectrum of (*E*)-**SA** (12.5 μM) upon heating and cooling in the temperature range between 310 and 370 K at a rate of 1.0 K/min (see Supporting Information for experimental details). The spectrum of (*E*)-**SA** at 310 K showed a characteristic absorption band with a maximum centered at 371 nm (Figure 2a), comparable to the spectrum of the aggregates in toluene.[63] Upon heating, the band at 371 nm decreased in intensity, accompanied by the formation of two new local maxima at 340 and 357 nm, resulting in a spectrum that closely resembles the one of monomeric (*E*)-**SA** dissolved in an organic solvent [e.g., dimethyl sulfoxide (DMSO)].[63] These changes indicate the disassembly of the supramolecular

DOI: 10.31635/ccschem.022.202201821
Citation: *CCS Chem.* **2022**, 4, 2212–2220
Link to VoR: https://doi.org/10.31635/ccschem.022.202201821

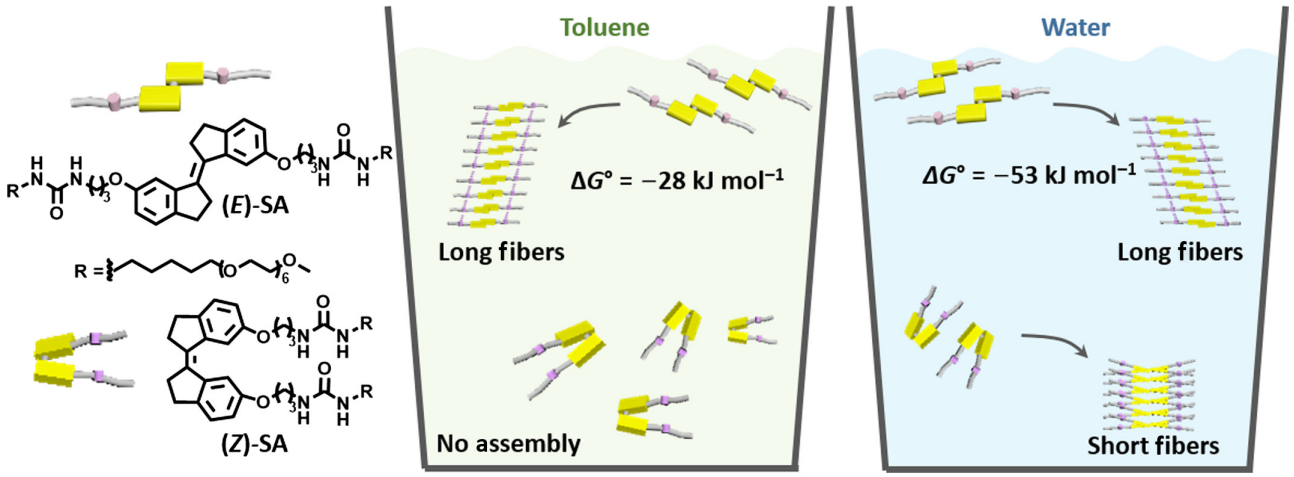

Figure 1 | *Molecular structure of **SA** and schematic illustrations of supramolecular polymerization of (E)-**SA** and (Z)-**SA** in toluene and water. Both assembly processes of (E)-**SA** follow an enthalpy-driven nucleation-elongation mechanism, where the Gibbs free energy (ΔG°) in water is double that in toluene. (Z)-**SA** is monomerically dissolved in toluene, where it forms short fibers in water.*

polymer during heating. Upon cooling from 370 to 310 K, the absorption maxima of (*E*)-**SA** at 340 and 357 nm gradually disappeared with concomitant formation of a band at 371 nm (Figure 2b), suggesting the transition from monomeric (*E*)-**SA** to well-defined aggregates. The temperature-dependent absorption of the aggregates at 371 nm showed a steep increase at a critical temperature of 358.5 K (inset in Figure 2b). The non-sigmoidal curve with a sharp transition at the critical temperature reflects a nucleation-elongation process.[53,67-69]

To identify the assembly structure, we performed cryo-transmission electron microscopy (TEM) measurements of the aggregates formed by (*E*)-**SA** in water. The images show nanofibers of hundreds of nanometers (≥500 nm) in length with a uniform diameter of 6.8 ± 0.5 nm (Figure 2c and Supporting Information Figure S1), indicating a well-defined 1D supramolecular polymer. To support the well-defined assembly in water, a hexamer formed by (*E*)-**SA** was modeled employing the GFN force field (GFN-FF).[70] A preliminary MD run of 100 ps at 398 K was performed using a Berendsen thermostat in implicit water (GBSA solvent model). The molecule was then optimized at the same level of theory (Figure 2d).[70,71] The (*E*)-stiff-stilbene core units stacked in a hexamer with a uniform distance of 3.5–4.0 Å, suggesting that the main forces that hold the molecules together at the nucleation stage are π-interactions between the stiff-stilbene cores, which are propagated along the fiber. While H-bonding between the ureas strengthens the interactions between the side chains of neighboring molecules in the final polymer, due to their random orientation, they seem to have a limited contribution at the nucleation stage. To study the role of hydrogen bonds in the assembly, we added different concentration of competing H-bond forming compounds into the aqueous solution of the supramolecular polymer formed by (*E*)-**SA** (5.0 μM) (Supporting Information Figure S9). The supramolecular polymers remained stable after adding 10^5 equiv of urea, evidenced by the consistent absorption at 371 nm of the well-defined aggregates (Supporting Information Figure S9a). Aiming to break the bis-urea hydrogen bonding, we also added formic acid as a stronger competing reagent (Supporting Information Figure S9b).[72] The supramolecular polymers remained stable even after adding 3×10^5 equiv of formic acid. The excellent stability of the bis-urea hydrogen bonding of our supramolecular polymer can be attributed to hydrophobic pockets formed by the C6 alkyl chain.[66,73] These results support our hypothesis that the increased stability of the supramolecular polymer of (*E*)-**SA** in water is thanks to hydrogen bonding that cannot be easily disrupted, even by adding an excess of competing reagent. Consequently, the favorable urea interactions, that is, H-bonding, facilitate the directional growth of supramolecular polymer in water.[49]

To study the polymerization mechanism, we recorded the absorption at λ = 371 nm for samples with increasing total concentration (c_T) of (*E*)-**SA** upon heating and cooling (Supporting Information Figures S4 and S5). The curves representing the degree of aggregation (α_{agg}, estimated from the absorption at λ = 371 nm) as a function of temperature are shown in Figures 3a and 3b. In the heating and cooling processes, the non-sigmoidal shape of the curves in combination with the intense transitions at the critical temperatures T_e and T_e' confirm a cooperative (nucleation-elongation) polymerization.[53,67-69] The higher critical temperature in the heating process (T_e) compared to the one in the cooling process (T_e') revealed a thermal hysteresis (Figure 3c), suggesting that the assembly

DOI: 10.31635/ccschem.022.202201821
Citation: *CCS Chem.* **2022**, 4, 2212–2220
Link to VoR: https://doi.org/10.31635/ccschem.022.202201821

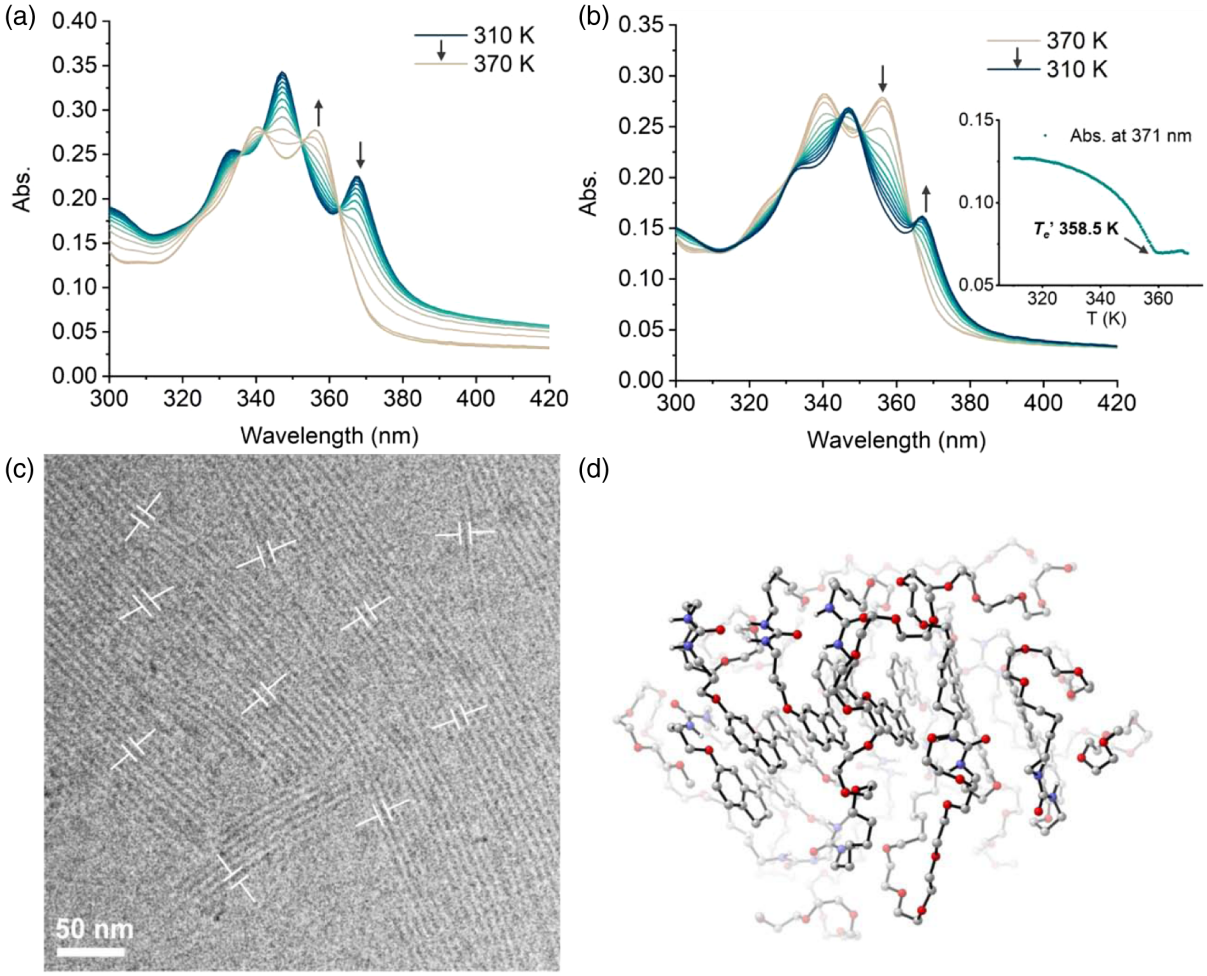

Figure 2 | *Temperature-dependent changes in the UV–vis absorption spectrum of (E)-**SA** (12.5 μM) in water during (a) heating from 310 to 370 K and (b) cooling from 370 to 310 K at a rate of 1.0 K/min. Inset: absorption at 371 nm. (c) Cryo-TEM image of (E)-**SA** (0.4 mM) in water. (d) Hexamer of (E)-**SA** optimized at the GFN-FF level in water.*

during the cooling process is under kinetic control.[68] In contrast, the heating-induced disassembly is under thermodynamic control, an observation confirmed by an unaltered T_e upon increasing the heating rate from 0.5 to 2 K·min^{-1} (Supporting Information Figure S6). We further analyzed the melting curve to obtain the thermodynamic parameters using the Van't Hoff plot.[68] The natural logarithm of c_T showed a linear relationship with the reciprocal T_e (Figure 3d). The standard enthalpy $\Delta H°$ = –124 kJ mol^{-1} is more negative than the one (–77 kJ mol^{-1}) obtained when using toluene as the solvent (Table 1). Possibly, the main contributions to $\Delta H°$ in toluene can be attributed to urea H-bonding and π–π stacking, while in water, the non-classical hydrophobic effect[74] leads to a more negative enthalpy.[45] The standard entropy ($\Delta S°$) in water is –244 J mol^{-1} K^{-1}, which is more negative than the –165 J mol^{-1} K^{-1} obtained for (*E*)-**SA** in toluene. The more organized hydrophobic core and the decrease in degrees of freedom of the side chains contribute to this enhanced negative value in water. As a result, the Gibbs free energy ($\Delta G°$ = –53 kJ mol^{-1}) of polymerization in water is almost double that in toluene, suggesting a more robust assembly in water.[49] The equilibrium constants of the supramolecular polymerization process in water and toluene are 2.8 × 10^9 M^{-1} and 9.8 × 10^4 M^{-1} (Table 1), respectively, obtained using the mass balance model developed by Markvoort et al.[75] The overall features suggest that the supramolecular polymerization of (*E*)-**SA** in water is an enthalpy-driven nucleation-elongation process with hydrophobic effects contributing significantly to $\Delta G°$.

(*E*)-**SA** gelated in water with a relatively low critical concentration (1 mg/mL), following a heating–cooling cycle (see Supporting Information Figure S3), whereas (*Z*)-**SA** failed to form a hydrogel under the same conditions. We also recorded cryo-TEM images of a hydrogel of (*E*)-**SA** (Supporting Information Figure S3), in which the concentration was higher than the above studied supramolecular polymer and where the sample had undergone an additional heating–cooling (annealing) process. The diameter and length of the fibers in the hydrogel were similar to

DOI: 10.31635/ccschem.022.202201821
Citation: *CCS Chem.* **2022**, 4, 2212–2220
Link to VoR: https://doi.org/10.31635/ccschem.022.202201821

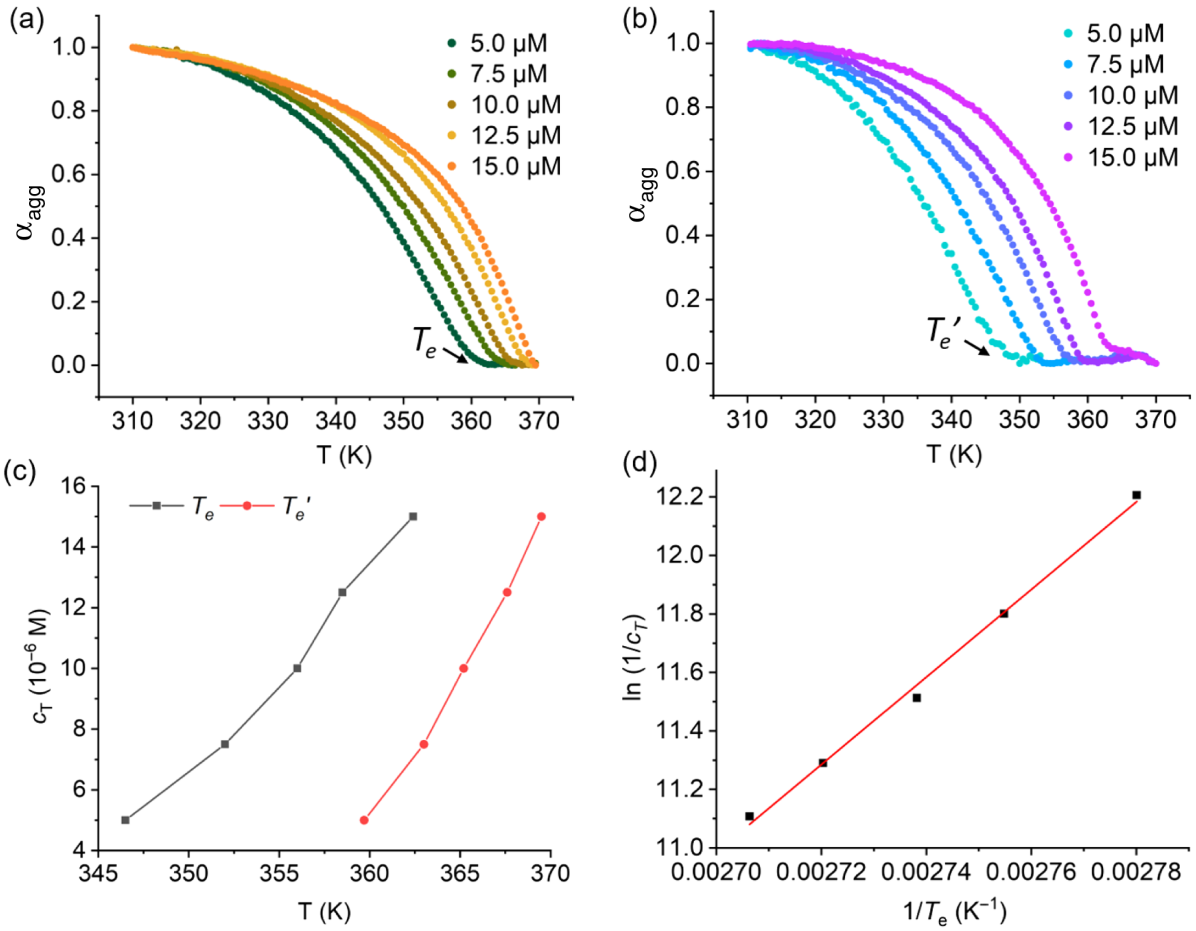

Figure 3 | *Temperature-dependent degree of aggregation (α_{agg}) of (E)-**SA** estimated from the apparent absorption coefficients at λ = 371 nm at different total concentrations (c_T) in water upon (a) heating and (b) cooling at a rate of 1.0 K/min. (c) Values of T_e and T_e' observed for (E)-**SA** at different c_T. (d) Natural logarithm of the reciprocal c_T as a function of the reciprocal T_e (Van't Hoff plot).*

the supramolecular polymer reported above (Supporting Information Figure S3 and Figure 2a), while their entanglement suggests the formation of a fibrous network that contributes to gelation. The photo-isomerization behavior of the hydrogel was studied by NMR (see Supporting Information Figure S7). After irradiating the sample for 30 min, the ^{1}H NMR spectrum remained the same, suggesting that the photo-isomerization of (*E*)-**SA** in the assembled (aggregate) state was possibly hampered in water at room temperature, but happed at a temperature higher than Te (Supporting Information Figures S7 and S10). By comparing with the system in toluene, where photo-isomerization of assembled (*E*)-**SA** is feasible,[63] we speculate that the reason for the impeded isomerization in water is a consequence of a stronger aggregation,[22] as evidenced by a $\Delta G°_{water}$ almost double that of $\Delta G°_{toluene}$. The strong aggregating abilities of (*E*)- and (*Z*)-**SA** in water were also evidenced by the broadened proton resonances in the ^{1}H NMR spectra (298 K, 500 MHz, D_2O) (Supporting Information Figure S17).[76]

To study the differences in the assembly of (*E*)- and (*Z*)-**SA**, we also measured the UV–vis absorption spectrum and cryo-TEM images for (*Z*)-**SA**. The UV–vis spectrum of (*Z*)-**SA** in water showed a hypsochromic shift compared with the one in DMSO (Figure 4a), suggesting the formation of aggregates in water. The cryo-TEM image of (*Z*)-**SA**

Table 1 | *Thermodynamic Parameters Describing the Assembly of* (E)-***SA*** *in Toluene and Water*

Solvent	$\Delta H°$ (kJ mol^{-1})	$\Delta S°$ (J mol^{-1} K^{-1})	$\Delta G°$ (293 K) (kJ mol^{-1})	K (293 K) (M^{-1})
Toluene	–77	–165	–28	9.8×10^4
Water	–124	–244	–53	2.8×10^9

DOI: 10.31635/ccschem.022.202201821
Citation: *CCS Chem.* **2022**, 4, 2212–2220
Link to VoR: https://doi.org/10.31635/ccschem.022.202201821

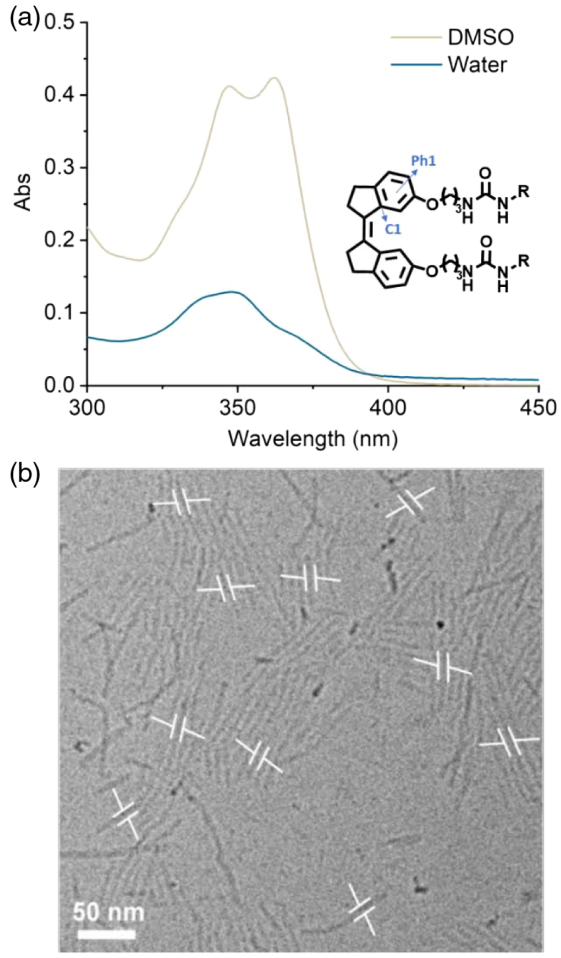

Figure 4 | *(a) UV–vis absorption spectra of (Z)-**SA** (10.0 μM) in DMSO and water. Inset: molecular structure of (Z)-**SA**. (b) Cryo-TEM image of (Z)-**SA** (0.4 mM) in water.*

in water revealed the formation of short fibers, with a length of approximately 50 nm and a diameter of 8.0 ± 0.6 nm (Figure 4b and Supporting Information Figure S2). These results are distinct from the ones in toluene, where (*Z*)-**SA** is monomeric due to the less planar structure and the formation of intramolecular instead of intermolecular hydrogen bonds.[63] The dihedral angle between the plane of phenyl group Ph1 and the plane formed by the ethylene and atom C1 is 14.3° (Figure 4a); hence, (*Z*)-**SA** is not planar and less susceptible to π–π stacking.[65] Therefore, the aggregation of (*Z*)-**SA** in water is mainly attributed to hydrophobic effects, and the shorter fiber length of (*Z*)-**SA** compared with (*E*)-**SA** might be related to the lack of π–π stacking and intermolecular hydrogen bonds. Although direct in situ control of assembly structure by irradiation is not feasible, external photochemical isomerization allows for controlling the length of the supramolecular fiber, achieving a tenfold difference with minimal changes in diameter.

Conclusions

The thermodynamic analysis of the supramolecular polymerization of (*E*)-**SA** in water revealed an enthalpy-driven nucleation-elongation process. Taking advantage of both the water and toluene adaptive supramolecular polymer of (*E*)-**SA**, we determined the impact of hydrophobic effects on the supramolecular polymerization in water by comparing the two systems. The hydrophobic effects were found to contribute significantly to $\Delta G°$, resulting in more robust fibers in water. Cryo-TEM studies on the 1D assemblies of (*E*)-**SA** and (*Z*)-**SA**, the former of which displays a more planar structure, indicate that the presence of favorable π–π interactions and intermolecular hydrogen bonds drastically increase the length of supramolecular polymers. The thermodynamic insights will enrich the fundamental understanding of aqueous supramolecular polymers, facilitating the design of supramolecular materials by a bottom-up strategy.

Supporting Information

Supporting Information is available and including sample preparation, characterization, UV–vis, cryo-TEM, NMR, and computational studies.

Conflict of Interest

There is no conflict of interest to report.

Funding Information

Financial support from the Netherlands Organization for Scientific Research (NWO-CW), the European Research Council (ERC; advanced grant no. 694345 to B.L.F.), the Dutch Ministry of Education, Culture and Science (Gravitation program no. 024.001.035), the China Scholarship Council (CSC; no. 201707040064 to F.X.), and the Marie Skłodowska-Curie Actions (Individual Fellowships no. 838280 to S.C. and no. 793082 to L.P.) is gratefully acknowledged.

Acknowledgments

The authors wish to acknowledge Dr. Sander J. Wezenberg and Dr. Franco King-Chi Leung for helpful discussions.

References

1. Lehn, J. M. *Supramolecular Chemistry*; John Wiley & Sons: Strasbourg, **1995**.
2. Brunsveld, L.; Folmer, B. J. B.; Meijer, E. W.; Sijbesma, R. P. Supramolecular Polymers. *Chem. Rev.* **2001**, *101*, 4071–4098.

DOI: 10.31635/ccschem.022.202201821
Citation: *CCS Chem.* **2022**, 4, 2212–2220
Link to VoR: https://doi.org/10.31635/ccschem.022.202201821

3. Aida, T.; Meijer, E. W.; Stupp, S. I. Functional Supramolecular Polymers. *Science* **2012**, *335*, 813–817.
4. de Greef, T. F. A.; Smulders, M. M. J.; Wolffs, M.; Schenning, A. P. H. J.; Sijbesma, R. P.; Meijer, E. W. Supramolecular Polymerization. *Chem. Rev.* **2009**, *109*, 5687–5754.
5. Schmuck, C.; Wienand, W. Self-Complementary Quadruple Hydrogen-Bonding Motifs as a Functional Principle: From Dimeric Supramolecules to Supramolecular Polymers. *Angew. Chem. Int. Ed.* **2001**, *40*, 4363–4369.
6. Dong, S.; Zheng, B.; Wang, F.; Huang, F. Supramolecular Polymers Constructed from Macrocycle-Based Host-Guest Molecular Recognition Motifs. *Acc. Chem. Res.* **2014**, *47*, 1982–1994.
7. Hartlieb, M.; Mansfield, E. D. H.; Perrier, S. A Guide to Supramolecular Polymerizations. *Polym. Chem.* **2020**, *11*, 1083–1110.
8. de Loos, M.; Feringa, B. L.; van Esch, J. H. Design and Application of Self-Assembled Low Molecular Weight Hydrogels. *Eur. J. Org. Chem.* **2005**, *2005*, 3615–3631.
9. Thompson, C. B.; Korley, L. S. T. J. 100th Anniversary of Macromolecular Science Viewpoint: Engineering Supramolecular Materials for Responsive Applications—Design and Functionality. *ACS Macro Lett.* **2020**, *9*, 1198–1216.
10. Clemons, T. D.; Stupp, S. I. Design of Materials with Supramolecular Polymers. *Prog. Polym. Sci.* **2020**, *111*, 101310.
11. Goor, O. J. G. M.; Hendrikse, S. I. S.; Dankers, P. Y. W.; Meijer, E. W. From Supramolecular Polymers to Multi-Component Biomaterials. *Chem. Soc. Rev.* **2017**, *46*, 6621–6637.
12. Mabesoone, M. F. J.; Palmans, A. R. A.; Meijer, E. W. Solute-Solvent Interactions in Modern Physical Organic Chemistry: Supramolecular Polymers as a Muse. *J. Am. Chem. Soc.* **2020**, *142*, 19781–19798.
13. Satake, A. The Solvent Effect on Weak Interactions in Supramolecular Polymers: Differences between Small Molecular Probes and Supramolecular Polymers. *Chempluschem* **2020**, *85*, 1542–1548.
14. Cremer, P. S.; Flood, A. H.; Gibb, B. C.; Mobley, D. L. Collaborative Routes to Clarifying the Murky Waters of Aqueous Supramolecular Chemistry. *Nat. Chem.* **2017**, *10*, 8–16.
15. Datta, S.; Saha, M. L.; Stang, P. J. Hierarchical Assemblies of Supramolecular Coordination Complexes. *Acc. Chem. Res.* **2018**, *51*, 2047–2063.
16. Chen, S.; Costil, R.; Leung, F. K. C.; Feringa, B. L. Self-Assembly of Photoresponsive Molecular Amphiphiles in Aqueous Media. *Angew. Chem. Int. Ed.* **2021**, *60*, 11604–11627.
17. Volarić, J.; Szymanski, W.; Simeth, N. A.; Feringa, B. L. Molecular Photoswitches in Aqueous Environments. *Chem. Soc. Rev.* **2021**, *50*, 12377–12449.
18. Coleman, A. C.; Beierle, J. M.; Stuart, M. C. A.; Maciá, B.; Caroli, G.; Mika, J. T.; van Dijken, D. J.; Chen, J.; Browne, W. R.; Feringa, B. L. Light-Induced Disassembly of Self-Assembled Vesicle-Capped Nanotubes Observed in Real Time. *Nat. Nanotechnol.* **2011**, *6*, 547–552.
19. Barclay, T. G.; Constantopoulos, K.; Matisons, J. Nanotubes Self-Assembled from Amphiphilic Molecules via Helical Intermediates. *Chem. Rev.* **2014**, *114*, 10217–10291.
20. Thota, B. N. S.; Urner, L. H.; Haag, R. Supramolecular Architectures of Dendritic Amphiphiles in Water. *Chem. Rev.* **2016**, *116*, 2079–2102.
21. Xu, F.; Pfeifer, L.; Stuart, M. C. A.; Leung, F. K. C.; Feringa, B. L. Multi-Modal Control over the Assembly of a Molecular Motor Bola-Amphiphile in Water. *Chem. Commun.* **2020**, *56*, 7451–7454.
22. Franken, L. E.; Wei, Y.; Chen, J.; Boekema, E. J.; Zhao, D.; Stuart, M. C. A.; Feringa, B. L. Solvent Mixing to Induce Molecular Motor Aggregation into Bowl-Shaped Particles: Underlying Mechanism, Particle Nature, and Application to Control Motor Behavior. *J. Am. Chem. Soc.* **2018**, *140*, 7860–7868.
23. van Dijken, D. J.; Chen, J.; Stuart, M. C. A.; Hou, L.; Feringa, B. L. Amphiphilic Molecular Motors for Responsive Aggregation in Water. *J. Am. Chem. Soc.* **2016**, *138*, 660–669.
24. Chen, S.; Chen, S.; Leung, F. K. C.; Stuart, M. C. A.; Wang, C.; Feringa, B. L. Dynamic Assemblies of Molecular Motor Amphiphiles Control Macroscopic Foam Properties. *J. Am. Chem. Soc.* **2020**, *142*, 10163–10172.
25. Draper, E. R.; Adams, D. J. Low-Molecular-Weight Gels: The State of the Art. *Chem* **2017**, *3*, 390–410.
26. Buerkle, L. E.; Rowan, S. J. Supramolecular Gels Formed from Multi-Component Low Molecular Weight Species. *Chem. Soc. Rev.* **2012**, *41*, 6089–6102.
27. Chivers, P. R. A.; Smith, D. K. Shaping and Structuring Supramolecular Gels. *Nat. Rev. Mater.* **2019**, *4*, 463–478.
28. Jones, C. D.; Steed, J. W. Gels with Sense: Supramolecular Materials That Respond to Heat, Light and Sound. *Chem. Soc. Rev.* **2016**, *45*, 6546–6596.
29. Panja, S.; Adams, D. J. Stimuli Responsive Dynamic Transformations in Supramolecular Gels. *Chem. Soc. Rev.* **2021**, *50*, 5165–5200.
30. Liu, Y.; Yu, Y.; Gao, J.; Wang, Z.; Zhang, X. Water-Soluble Supramolecular Polymerization Driven by Multiple Host-Stabilized Charge-Transfer Interactions. *Angew. Chem. Int. Ed.* **2010**, *49*, 6576–6579.
31. Ma, X.; Tian, H. Stimuli-Responsive Supramolecular Polymers in Aqueous Solution. *Acc. Chem. Res.* **2014**, *47*, 1971–1981.
32. Krieg, E.; Bastings, M. M. C.; Besenius, P.; Rybtchinski, B. Supramolecular Polymers in Aqueous Media. *Chem. Rev.* **2016**, *116*, 2414–2477.
33. Hendrikse, S. I. S.; Su, L.; Hogervorst, T. P.; Lafleur, R. P. M.; Lou, X.; van der Marel, G. A.; Codee, J. D. C.; Meijer, E. W. Elucidating the Ordering in Self-Assembled Glycocalyx Mimicking Supramolecular Copolymers in Water. *J. Am. Chem. Soc.* **2019**, *141*, 13877–13886.
34. Helmers, I.; Ghosh, G.; Albuquerque, R. Q.; Fernández, G. Pathway and Length Control of Supramolecular Polymers in Aqueous Media via a Hydrogen Bonding Lock. *Angew. Chem. Int. Ed.* **2020**, 4368–4376.
35. Fuentes, E.; Gerth, M.; Berrocal, J. A.; Matera, C.; Gorostiza, P.; Voets, I. K.; Pujals, S.; Albertazzi, L. An Azobenzene-Based Single-Component Supramolecular Polymer Responsive to Multiple Stimuli in Water. *J. Am. Chem. Soc.* **2020**, *142*, 10069–10078.

DOI: 10.31635/ccschem.022.202201821
Citation: *CCS Chem.* **2022**, 4, 2212–2220
Link to VoR: https://doi.org/10.31635/ccschem.022.202201821

36. Yin, Z.; Song, G.; Jiao, Y.; Zheng, P.; Xu, J. F.; Zhang, X. Dissipative Supramolecular Polymerization Powered by Light. *CCS Chem.* **2019**, *1*, 335–342.
37. Dong, R.; Zhou, Y.; Huang, X.; Zhu, X.; Lu, Y.; Shen, J. Functional Supramolecular Polymers for Biomedical Applications. *Adv. Mater.* **2015**, *27*, 498–526.
38. Biswas, S.; Kinbara, K.; Niwa, T.; Taguchi, H.; Ishii, N.; Watanabe, S.; Miyata, K.; Kataoka, K.; Aida, T. Biomolecular Robotics for Chemomechanically Driven Guest Delivery Fuelled by Intracellular ATP. *Nat. Chem.* **2013**, *5*, 613–620.
39. Chen, J.; Leung, F. K. C.; Stuart, M. C. A.; Kajitani, T.; Fukushima, T.; van der Giessen, E.; Feringa, B. L. Artificial Muscle-Like Function from Hierarchical Supramolecular Assembly of Photoresponsive Molecular Motors. *Nat. Chem.* **2018**, *10*, 132–138.
40. Leung, F. K. C.; van den Enk, T.; Kajitani, T.; Chen, J.; Stuart, M. C. A.; Kuipers, J.; Fukushima, T.; Feringa, B. L. Supramolecular Packing and Macroscopic Alignment Controls Actuation Speed in Macroscopic Strings of Molecular Motor Amphiphiles. *J. Am. Chem. Soc.* **2018**, *140*, 17724–17733.
41. Leung, F. K.; Kajitani, T.; Stuart, M. C. A.; Fukushima, T.; Feringa, B. L. Dual-Controlled Macroscopic Motions in a Supramolecular Hierarchical Assembly of Motor Amphiphiles. *Angew. Chem. Int. Ed.* **2019**, *58*, 10985–10989.
42. Allampally, N. K.; Florian, A.; Mayoral, M. J.; Rest, C.; Stepanenko, V.; Fernández, G. H-Aggregates of Oligophenyleneethynylene (OPE)-BODIPY Systems in Water: Guest Size-Dependent Encapsulation Mechanism and Co-Aggregate Morphology. *Chem. Eur. J.* **2014**, *20*, 10669–10678.
43. Rödle, A.; Lambov, M.; Mück-Lichtenfeld, C.; Stepanenko, V.; Fernández, G. Cooperative Nanoparticle H-Type Self-Assembly of a Bolaamphiphilic BODIPY Derivative in Aqueous Medium. *Polymer* **2017**, *128*, 317–324.
44. Lafleur, R. P. M.; Schoenmakers, S. M. C.; Madhikar, P.; Bochicchio, D.; Baumeier, B.; Palmans, A. R. A.; Pavan, G. M.; Meijer, E. W. Insights into the Kinetics of Supramolecular Comonomer Incorporation in Water. *Macromolecules* **2019**, *52*, 3049–3055.
45. Syamala, P. P. N.; Würthner, F. Modulation of the Self-Assembly of π-Amphiphiles in Water from Enthalpy- to Entropy-Driven by Enwrapping Substituents. *Chem. Eur. J.* **2020**, *26*, 8426–8434.
46. Görl, D.; Würthner, F. Entropically Driven Self-Assembly of Bolaamphiphilic Perylene Dyes in Water. *Angew. Chem. Int. Ed.* **2016**, *55*, 12094–12098.
47. Baker, M. B.; Albertazzi, L.; Voets, I. K.; Leenders, C. M. A.; Palmans, A. R. A.; Pavan, G. M.; Meijer, E. W. Consequences of Chirality on the Dynamics of a Water-Soluble Supramolecular Polymer. *Nat. Commun.* **2015**, *6*, 6234.
48. Bochicchio, D.; Pavan, G. M. From Cooperative Self-Assembly to Water-Soluble Supramolecular Polymers Using Coarse-Grained Simulations. *ACS Nano* **2017**, *11*, 1000–1011.
49. Garzoni, M.; Baker, M. B.; Leenders, C. M. A.; Voets, I. K.; Albertazzi, L.; Palmans, A. R. A.; Meijer, E. W.; Pavan, G. M. Effect of H-Bonding on Order Amplification in the Growth of a Supramolecular Polymer in Water. *J. Am. Chem. Soc.* **2016**, *138*, 13985–13995.
50. Rest, C.; Mayoral, M. J.; Fucke, K.; Schellheimer, J.; Stepanenko, V.; Fernández, G. Self-Assembly and (Hydro) Gelation Triggered by Cooperative π-π And Unconventional C-H···X Hydrogen Bonding Interactions. *Angew. Chem. Int. Ed.* **2014**, *53*, 700–705.
51. Syamala, P. P. N.; Soberats, B.; Görl, D.; Gekle, S.; Würthner, F. Thermodynamic Insights into the Entropically Driven Self-Assembly of Amphiphilic Dyes in Water. *Chem. Sci.* **2019**, *10*, 9358–9366.
52. Casellas, N. M.; Pujals, S.; Bochicchio, D.; Pavan, G. M.; Torres, T.; Albertazzi, L.; García-Iglesias, M. From Isodesmic to Highly Cooperative: Reverting the Supramolecular Polymerization Mechanism in Water by Fine Monomer Design. *Chem. Commun.* **2018**, *54*, 4112–4115.
53. Aratsu, K.; Takeya, R.; Pauw, B. R.; Hollamby, M. J.; Kitamoto, Y.; Shimizu, N.; Takagi, H.; Haruki, R.; Adachi, S.; Yagai, S. Supramolecular Copolymerization Driven by Integrative Self-Sorting of Hydrogen-Bonded Rosettes. *Nat. Commun.* **2020**, *11*, 1623.
54. Villarón, D.; Wezenberg, S. J. Stiff-Stilbene Photoswitches: From Fundamental Studies to Emergent Applications. *Angew. Chem. Int. Ed.* **2020**, *59*, 13192–13202.
55. Wezenberg, S. J.; Feringa, B. L. Photocontrol of Anion Binding Affinity to a Bis-Urea Receptor Derived from Stiff-Stilbene. *Org. Lett.* **2017**, *19*, 324–327.
56. Wezenberg, S. J.; Feringa, B. L. Supramolecularly Directed Rotary Motion in a Photoresponsive Receptor. *Nat. Commun.* **2018**, *9*, 1984.
57. Sheng, J.; Crespi, S.; Feringa, B. L.; Wezenberg, S. J. Supramolecular Control of Unidirectional Rotary Motion in a Sterically Overcrowded Photoswitchable Receptor. *Org. Chem. Front.* **2020**, *7*, 3874–3879.
58. Costil, R.; Crespi, S.; Pfeifer, L.; Feringa, B. L. Modulation of a Supramolecular Figure-of-Eight Strip Based on a Photoswitchable Stiff-Stilbene. *Chem. Eur. J.* **2020**, *26*, 7783–7787.
59. Yang, Q. Z.; Huang, Z.; Kucharski, T. J.; Khvostichenko, D.; Chen, J.; Boulatov, R. A Molecular Force Probe. *Nat. Nanotechnol.* **2009**, *4*, 302–306.
60. Wu, Y. H.; Huang, K.; Chen, S. F.; Chen, Y. Z.; Tung, C. H.; Wu, L. Z. Stiff-Stilbene Derivatives as New Bright Fluorophores with Aggregation-Induced Emission. *Sci. China Chem.* **2019**, *62*, 1194–1197.
61. Ogawa, K.; Harada, J.; Tomoda, S. Unusually Short Ethylene Bond and Large Amplitude Torsional Motion of (E)-stilbenes in Crystals. X-ray Crystallographic Study of "stiff" Stilbenes. *Acta Crystallogr. Sect. B* **1995**, *51*, 240–248.
62. Wang, Y.; Sun, C. L.; Niu, L. Y.; Wu, L. Z.; Tung, C. H.; Chen, Y. Z.; Yang, Q. Z. Photoresponsive AA/BB Supramolecular Polymers Comprising Stiff-Stilbene Based Guests and Bispillar[5]Arenes. *Polym. Chem.* **2017**, *8*, 3596–3602.
63. Xu, F.; Pfeifer, L.; Crespi, S.; Leung, F. K. C.; Stuart, M. C. A.; Wezenberg, S. J.; Feringa, B. L. From Photoinduced Supramolecular Polymerization to Responsive Organogels. *J. Am. Chem. Soc.* **2021**, *143*, 5990–5997.
64. Xu, J. F.; Chen, Y. Z.; Wu, D.; Wu, L. Z.; Tung, C. H.; Yang, Q. Z. Photoresponsive Hydrogen-Bonded Supramolecular Polymers Based on a Stiff Stilbene Unit. *Angew. Chem. Int. Ed.* **2013**, *52*, 9738–9742.

DOI: 10.31635/ccschem.022.202201821
Citation: *CCS Chem.* **2022**, 4, 2212–2220
Link to VoR: https://doi.org/10.31635/ccschem.022.202201821

65. Harada, J.; Ogawa, K.; Tomoda, S. "Stiff" Cis-Stilbenes. (Z)-6,6'-Dimethyl-1,1'-Biindanylidene and (Z)-4,4',7,7'-Tetramethyl-1,1'-Biindanylidene. *Acta Crystallogr. Sect. C Cryst. Struct. Commun.* **1995**, *51*, 2125–2127.
66. Obert, E.; Bellot, M.; Bouteiller, L.; Andrioletti, F.; Lehen-Ferrenbach, C.; Boué, F. Both Water- and Organo-Soluble Supramolecular Polymer Stabilized by Hydrogen-Bonding and Hydrophobic Interactions. *J. Am. Chem. Soc.* **2007**, *129*, 15601–15605.
67. Jonkheijm, P.; Van Der Schoot, P.; Schenning, A. P. H. J.; Meijer, E. W. Probing the Solvent-Assisted Nucleation Pathway in Chemical Self-Assembly. *Science* **2006**, *313*, 80–83.
68. Ogi, S.; Stepanenko, V.; Sugiyasu, K.; Takeuchi, M.; Würthner, F. Mechanism of Self-Assembly Process and Seeded Supramolecular Polymerization of Perylene Bisimide Organogelator. *J. Am. Chem. Soc.* **2015**, *137*, 3300–3307.
69. Smulders, M. M. J.; Nieuwenhuizen, M. M. L.; de Greef, T. F. A.; van der Schoot, P.; Schenning, A. P. H. J.; Meijer, E. W. How to Distinguish Isodesmic from Cooperative Supramolecular Polymerisation. *Chem. Eur. J.* **2010**, *16*, 362–367.
70. Spicher, S.; Grimme, S. Robust Atomistic Modeling of Materials, Organometallic, and Biochemical Systems. *Angew. Chem. Int. Ed.* **2020**, *59*, 15665–15673.
71. Bannwarth, C.; Caldeweyher, E.; Ehlert, S.; Hansen, A.; Pracht, P.; Seibert, J.; Spicher, S.; Grimme, S. Extended Tight-Binding Quantum Chemistry Methods. *Wiley Interdiscip. Rev. Comput. Mol. Sci.* **2021**, *11*, 1–49.
72. Lloyd, G. O.; Steed, J. W. Anion-Tuning of Supramolecular Gel Properties. *Nat. Chem.* **2009**, *1*, 437–442.
73. Leenders, C. M. A.; Albertazzi, L.; Mes, T.; Koenigs, M. M. E.; Palmans, A. R. A.; Meijer, E. W. Supramolecular Polymerization in Water Harnessing Both Hydrophobic Effects and Hydrogen Bond Formation. *Chem. Commun.* **2013**, *49*, 1963–1965.
74. Biedermann, F.; Nau, W. M.; Schneider, H. J. The Hydrophobic Effect Revisited - Studies with Supramolecular Complexes Imply High-Energy Water as a Noncovalent Driving Force. *Angew. Chem. Int. Ed.* **2014**, *53*, 11158–11171.
75. Ten Eikelder, H. M. M.; Markvoort, A. J.; De Greef, T. F. A.; Hilbers, P. A. J. An Equilibrium Model for Chiral Amplification in Supramolecular Polymers. *J. Phys. Chem. B* **2012**, *116*, 5291–5301.
76. Xu, J. F.; Niu, L. Y.; Chen, Y. Z.; Wu, L. Z.; Tung, C. H.; Yang, Q. Z. Hydrogen Bonding Directed Self-Assembly of Small-Molecule Amphiphiles in Water. *Org. Lett.* **2014**, *16*, 4016–4019.

DOI: 10.31635/ccschem.022.202201821
Citation: *CCS Chem.* **2022**, 4, 2212–2220
Link to VoR: https://doi.org/10.31635/ccschem.022.202201821